ACTA METALLURGICA SLOVACA
2021, VOL. 27, NO. 4, 210-213

RESEARCH PAPER

FORMING PROCESS SIMULATION OF BIMETALLIC BILLET BY EXTRUSION FOR REW METHOD

Alexander Schrek[1], Alena Brusilová[1], Pavol Sejč[1], Branislav Vanko[1]

[1]Slovak University of Technology in Bratislava, Námestie slobody 17, 812 31 Bratislava, Slovak Republic, EU

[*] Corresponding author: alexander.schrek@stuba.sk, tel. +42157296207, Slovak University of Technology in Bratislava, Námestie slobody 17, 812 31 Bratislava, Slovak Republic, EU

Received: 03.11.2021
Accepted: 04.12.2021

ABSTRACT

The bimetallic joining elements were designed for lap joints of thin metallic (Fe-Fe, Fe-Al) as well as metallic – nonmetallic (Fe-PMMA, Al-PMMA) sheets by Resistance Element Welding (REW). The Cu tubes with an outer diameter of 4 mm, wall thickness of 0.5 mm, and a length of 11 mm filled with a solder Sn60Pb40 were used for the bimetallic joining elements producing. The required shape of joining elements is obtained by cold forming. Simulation by ANSYS software was chosen for the optimization of the forming process and geometry of functional parts of the forming tool allowing to use only one extrusion forming operation. The simulation results are stresses, strains, and modification of cross-section geometry of elements for the three proposed forming modes. The geometry of functional parts of the forming tool was compared with the results of cross-section macroanalysis of joining elements. Furthermore, REW joints of the selected material combinations that were subjected to macroanalysis are presented.

Keywords: extrusion, strain, simulation, forming tool, Resistance Element Welding

INTRODUCTION

Resistance Element Welding (REW) is one of the new joining methods applicable for joining the blanks of metallurgically unjoinable materials (Al-Fe, Plastic-Fe) [1 - 4]. This method is intended to create lap joints. The principle is based on the heating of the joining element (rivet) between the connected blanks by resistance heating which leads to the creating of metallurgical joint (**Fig. 1**). To create a joint, it is possible to use standard technical accessories (welding gun) intended for resistance spot welding (RSW) of the steel blanks [4, 5]. Correct joint geometry and the joining element dimensions, as well as a chemical composition of the material for its creation, have a significant influence on the required mechanical properties of the (REW) joint [6, 7]. During joining steel to aluminium, the joining element end is brazed to the steel blank while the aluminium blank is bonded in a joint only through the mechanical wedging. The fusion welding joint is created between the joining element and the blank along the whole circumference. The joining element can be made of the aluminium alloy. The problem that occurs in this solution is in splashing of the melted material of the head of the joining element, which causes worse functional and aesthetic joint characteristics. Another solution is using of a bimetallic joining element where the melting temperature of the cover material is higher than the melting temperature of the core. A material combination of the Cu tube (99.9 % Cu) cover with the outer diameter of 4 mm and the wall thickness of 0.5 mm, and the Sn60Pb40 solder core was suggested [8]. Molten Sn60Pb40 solder was poured into a hot Cu tube embedded in a graphite shell against an unheated graphite plate (**Fig. 2**). The casting temperature and the preheating temperature of the Cu tube in graphite shell were about 210 ° C. Prior to casting, a soldering flux was applied into the Cu tube to remove surface oxides and improve the wettability [8-10]. For the desired dimensions of the joining element used for the REW (Fig. 1), the billet created from a bimetallic bar (Cu tube filled with a Sn60Pb40 solder) divided in the length of 11 mm was used.

The cold forming process was chosen for the joining element production. The head forming is possible to realize in several ways. The goal was to find such a solution that allows us to achieve a desired shape in one forming operation, without formation of defects [11-14]. The shape of the head was chosen in three variations as a flat shape (**Fig. 3a**), a concave shape at an angle of +10 degrees (**Fig. 3b**), and a convex shape at an angle of -10 degrees (**Fig. 3c**).

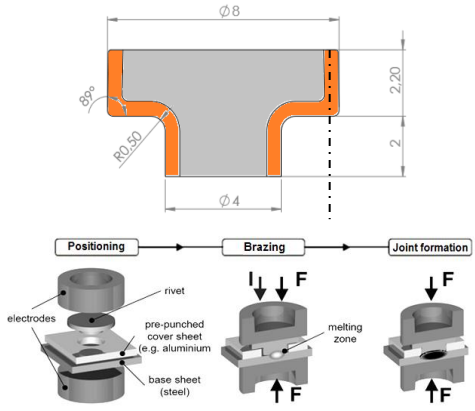

Fig. 1 The joining element and the principle of Resistance Element Welding [2]

Fig. 4 shows REW joint with significant defects of the joining element in the form of massive wrinkles. The pores appeared in the solder, but this is a metallurgical problem that wasn´t a subject of this examination. As a solution of the problem of wrinkle creation, the different geometries of punch which provide better material flow regulation as well as a mutual motion of a billet and a tool during the head formation, were designed [15-17]. The original method of element manufacturing used an upsetting process where the proposed and confirmed process was based on the motion of billet against a punch creating the head of the element. Computer simulations and practical experiments were used for a verification of the proposed alterations [18-20].

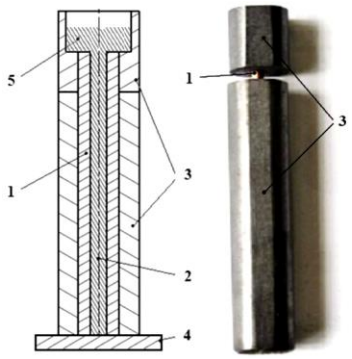

Fig. 2 Casting of bimetallic bar (1 - Cu tube, 2 - Sn60Pb40 solder, 3 - graphite shell, 4 - graphite plate, 5 – pouring cup)

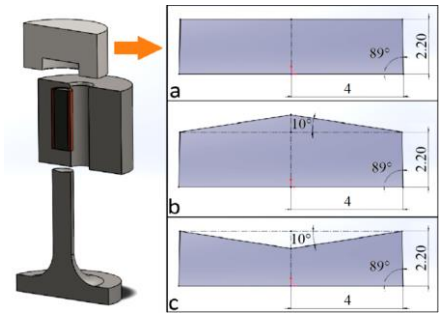

Fig. 3 Types (shapes) of element heads: a) flat, b) concave, c) convex

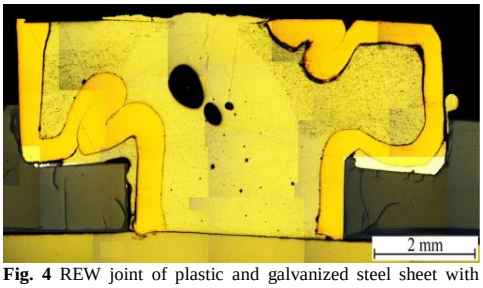

Fig. 4 REW joint of plastic and galvanized steel sheet with defects in the form of wrinkles and porosity in the joining element

MATERIAL AND METHODS

Material properties of joining element

The stress-strain characteristics of both materials of the bimetallic billet were used as the boundary conditions for the simulation of element head formation except the model of tool geometry. They were determined using the tensile testing machine INSTRON 1195 (**Table 1**).

Table 1 Stress-strain characteristics of joining element materials

Material	Density ($g.cm^{-3}$)	Yield strength *Re* (MPa)	Tensile strength *Rm* (MPa)	Elongation A_{Re} (%)
Cu	8.96	293	347.5	0.2
Sn60Pb40	8.5	40.2	61.5	1.3
Material	**Elongation A_{Rm} (%)**	**Young Modulus E (GPa)**	**Poisson ratio ν (-)**	**Tangent Modulus E_t (MPa)**
Cu	3.6	146	0.35	1602.94
Sn60Pb40	10.8	30.1	0.38	224.32

Simulation of technological process

For stresses and strains, simulation of bimetal and overall strains and shape of the element (billet), software ANSYS 18.2 was used. The tool model was created in CATIA VSR20 software. The billet motion velocity v = 2.67 mm·s^{-1}, friction coefficient f = 0.1, the element dimension of meshing function (meshing size) = 0.25 mm, temperature T = 20 °C, the definition of bimetal border line through the use of rough function, together with the tool geometry and stress-strain characteristics of materials, were used as the boundary conditions. The model of a simulation is illustrated in **Fig. 5**. The head forming is performed by the motion of a bottom punch together with the billet up to the head die.

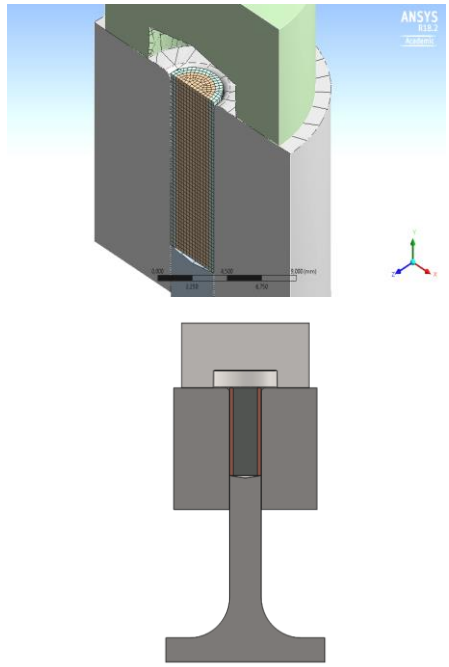

Fig. 5 The model of the tool (die) with billet for simulation

The values and distribution of stresses during the forming of the element head are illustrated in **Fig. 6**. According to the simulation, it is necessary to obtain stresses down to 2 250 MPa for complete filling of the die cavity and the bottom corners of head. There were found no indications of wrinkle formation in simulations. The stresses development depending on a stroke and time for head shape alternatives is documented in **Fig. 7**.

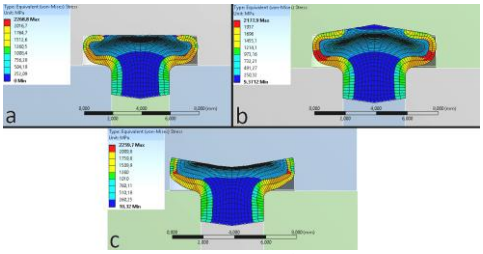

Fig. 6 The distribution and values of stresses in a bimetallic billet during the forming of three different head shapes: a) flat, b) concave, c) convex

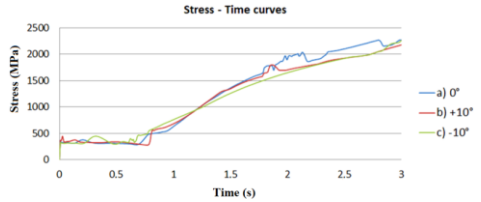

Fig. 7 The stresses development during the forming process for various alternatives

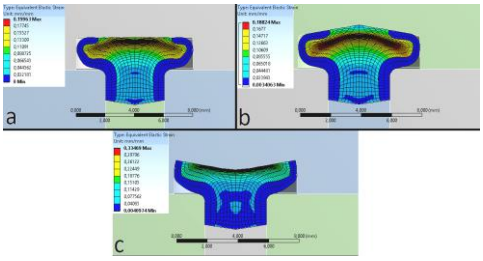

Fig. 8 The strain development in a bimetallic billet during the forming of three different head shapes: a) flat, b) concave, c) convex

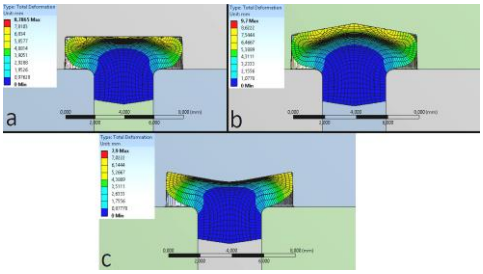

Fig. 9 The overall strain development in a bimetallic billet during the forming of three different head shapes: a) flat, b) concave, c) convex

The strain values and distribution in the bimetallic element during the head formation are shown in **Fig. 8**. The largest strain values were obtained at the point of the biggest change of a cross-section. The strain of Cu tube (a wall thickness reducing and increasing) corresponds to changes of the diameter cross-sections. The overall strain values and distribution in the element during the head formation are shown in **Fig. 9**. The biggest strain was at the point of the biggest change of the diameter cross-sections. There was zero strain in shank.

RESULTS AND DISCUSSION

The joining elements were formed in a tool with replaceable punches shaping the head face into a straight, concave, and convex shape. The single-acting hydraulic press DP1600, the maximum forming force was 25 kN. To evaluate the forming process, the elements cross-sections were made and subjected to macroscopic analysis with focusing on a tube deformation, wrinkle formation, and overall symmetry (**Fig. 10**). The elements 10a and 10b are characterized by good symmetry, only with a small indication of wrinkle formation. The element 10c has a greater asymmetry due to more pronounced wrinkles. However, in comparison with the initial experiments, for the forming of the head by upsetting, this shape is also acceptable. The resulting shape imperfections were caused by inaccuracies in the preparation of billets. During their production - cutting to the required length, it is necessary to keep the parallelism of the front surfaces. The non-parallelism of the surfaces is resulted in nonconstant plastic flow. The realized extrusion procedure significantly eliminated or totally removed the formation of wrinkles in the forming of the head of the joining elements, documented at the beginning of the paper. The structure of the solder wasn´t characterized by a postforming texture but by a dendritic structure. This structure was formed during the production of samples for macroanalysis by pressing into a thermoplastic at a temperature of about 190 °C. Pre-crystallization process affected the final solder structure. When using joining elements to form REW joints, it can be assumed that the most suitable head shape will be flat or convex (**Fig. 10a** and **10c**). In the concave head shape (**Fig. 10b**), the electrode comes into contact with the solder and due to the pressing force and the heat from the electric current transfer, the solder will be spurted out.

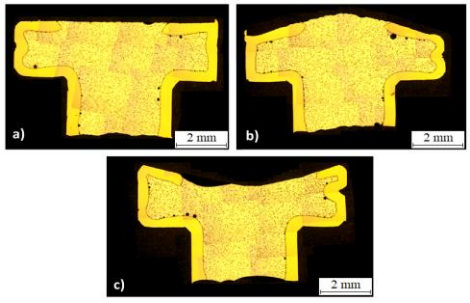

Fig. 10 The macrostructure of joining elements: a) flat, b) concave, c) convex

CONCLUSION

Resistance Element Welding (REW) is an appropriate method for creating lap joints of dissimilar materials, e.g., Al-Fe or Plastic-Fe. The joint is created through the joining element by brazing or soldering, not by welding, what affects the lower heat influence of the joint. The experiments showed that the joining element had to be solved in bimetallic form. This solution eliminated the splash problem of the joining element

material, which decreased functional and aesthetic joint characteristics. The goal of the joining elements production was to create a product with minimum defects like asymmetry of solder and Cu tube, as well as massive wrinkles of Cu tube which negatively affect the joining process. The joining elements were made of a billet that was made from a thin-walled Cu tube filled with Sn60Pb40 solder. From many types of cold forming processes for head shaping, the single-function technological process was chosen and confirmed by simulation. This procedure eliminates the buckling stiffness problem of the free billet part causing undesired wrinkle formation. The stress-strain characteristics of bimetallic material determined by mechanical testing were used in the ANSYS 18.2 simulation software. The tool model with different geometries of the head forming die was part of the simulation process. The simulation and experiment results confirmed the accuracy of the proposed technological process. This procedure will be used for the designing of the progressive tool, which will be used for cutting of bimetallic bar to the length of billets and forming of the joining elements. The proposed and verified method of bimetallic billet production will be also used for other product dimensions.

ACKNOWLEDGEMENTS

This work was supported by the Slovak grant agency VEGA for the financial support of the project VEGA 1/0405/19 and University Science Park STU Bratislava ITMS code 26240220084.

REFERENCES

1. G. Meschut, Ch. Schmal, T. Olfermann: Welding in the World, 61(3), 2017, 435-442. https://doi.org/10.1007/s40194-017-0431-3.
2. H. Zhang, J. Senkara: *Resistance Welding. Fundamentals and Applications*, 2nd Edition, CRC Press, New York, 2005.
3. J. Kang, H. M. Rao, D. R. Sigler, B. E. Carlson: Procedia Structural Integrity, 5, 2017, 1425-1432. https://doi.org/10.1016/j.prostr.2017.07.207.
4. J. Chen, X. Yuan, Z. Hu, Ch. Sun, Y. Zhang, Y. Zhang: Materials Characterization, 120, 2016, 45–52. https://doi.org/10.1016/j.matchar.2016.08.015.
5. L. Cui, R. Qiub, L. Hou，Z. Shen，Q. Li: Resistance Spot Welding between Steel and Aluminum Alloy. In.: *5th International Conference on Advanced Design and Manufacturing Engineering*, Atlantis Press, 2015, p. 777-781. http://doi.org/10.2991/icadme-15.2015.152.
6. G. Meschut, O. Hahn, V. Janzen. T. Olfermann: Welding in the World, 58(1), 2014, 65-75. https://doi.org/10.1007/s40194-013-0098-3.
7. G. Meschut, V. Janzen, T. Olfermann: Journal of Materials Engineering and Performance, 23(5), 2014, 1515-1523. https://doi.org/10.1007/s11665-014-0962-3.
8. N. Santoso, B. Suharnadi, B. T. Prayoga, L. D. Setyana: Acta Metallurgica Slovaca, 27(1), 2021, 28-31. https://doi.org/10.36547/ams.27.1.756.
9. L. D. Setyana, M. Mahardika, S. Suyitno: Acta Metallurgica Slovaca, 25(3), 2019, 193-202. https://doi.org/10.12776/ams.v25i3.1315.
10. L. D. Setyana, M. Mahardika, S. Suyitno: Acta Metallurgica Slovaca, 26(3), 2020, 132-137. https://doi.org/10.36547/ams.26.3.535.
11. A. Khrosravifard, R. Ebrahimi: Materials & Design, 31(1), 2010, 493-499. https://doi.org/10.1016/j.matdes.2009.06.026.
12. S. Z. Qamar, T. Pervez, J. Ch. Chekotu: Metals, 8(6), 2018, 1-18. http://doi.org/10.3390/met8060380.
13. P. Kazanowski, M. E. Epler, W. Z. Misiolek: Materials Science and Engineering, 369(1-2), 2004, 170-180. https://doi.org/10.1016/j.msea.2003.11.002.
14. S.Z Qamar, A.K. Sheikh, A.F.M. Arif, T. Pervez: Materials and Manufacturing Processes, 22(7-8), 2007, 804-810. https://doi.org/10.1080/10426910701446689.
15. H. Haghighat, M. M. Mahdavi: Transactions of Nonferrous Metals Society of China, 23(11), 2013, 3392-3399. https://doi.org/10.1016/S1003-6326(13)62879-4.
16. S. T. Oyinboa, T. Ch. Jena, S. O. Ismail: Engineering Solid Mechanics, 8, 2020, 205-214. https://doi.org/10.5267/j.esm.2020.1.003.
17. M. O. Mutlu, C. G. Guleryuz, Z. Parlar: IOP Conference Series: Materials Science and Engineering, 174, 2017, 012046. http://dx.doi.org/10.1088/1757-899X/174/1/012046.
18. X.-C. Zhuang, H. Xiang, Z. Zhao: International Journal of Automation and Computing, 7(3), 2010, 295-302. https://doi.org/10.1007/s11633-010-0506-8.
19. P. F. Zheng, L. C. Chan, T. C. Lee: Finite Elements in Analysis and Design, 42(3), 2005, 189-207. https://doi.org/10.1016/j.finel.2005.06.002.
20. T. Bakhtiani, H. El-Mounayri, J. Zhang: Materials Today Proceedings, 1(1), 2014, 94-106. https://doi.org/10.1016/j.matpr.2014.09.018.